2010 IEEE International Conference on Robotics and Automation
Anchorage Convention District
May 3-8, 2010, Anchorage, Alaska, USA

# Force Analysis and Path Planning of the Trapped Cell in Robotic Manipulation with Optical Tweezers

Yanhua Wu, Youhua Tan, Dong Sun, and Wenhao Huang

*Abstract*—**Laser trapping in the near infrared regime is a noninvasive and convenient manipulation tool, which can be utilized as micromanipulator for a large number of biological applications. Increasing demands for both accuracy and efficiency in cell manipulation highlight the need for automation process that integrates robotics and tweezers technologies. In this paper, we propose a robotic manipulation system with optical tweezers, and analyze the force applied on the trapped cell for design of an optimal trapping strategy. The dynamic motion of the cell with consideration of both the trapping and the viscous forces is analyzed, based on which the motion profile of the motorized stage is designed to ensure both safety and efficiency of the cell delivery. A modified A-star algorithm is used for path planning in transporting cells. Experiments are performed on manipulating the yeast cells to demonstrate the effectiveness of the proposed approach.**

## I. Introduction

Physical manipulation of biological cells or organelle plays an important role in experimental cell biology and immunology of biomedical research. Flow sorting and mechanical micromanipulation have been used widely for cell separation and positioning. Flow sorters divert a batch of cells in a volume of fluid, and thus have limited positional accuracy. Mechanical manipulators (such as the micro pipette) can position the selected cell with micron accuracy but induce damage to the cells and require relatively large open volumes for unhindered operation. Optical forces from a tightly focused laser beam can be used to confine and manipulate microscopic particles [1], both as actuators and sensors [2]. Optical trapping is based on the transfer of momentum between microscopic particles and the photons they scatter. A dielectric particle near the focus of the beam suffers from a force due to the transfer of momentum by scattering incident photons [1]. Optical trap exploits the force to precisely manipulate fine particles without mechanical contact, and thus produces less damage to biological objects (with proper laser power and wavelength) than the mechanical methods [2-3]. It can also function in a completely enclosed system with a small size. The optical trap has been applied to a variety of research areas, such as micro-manipulation for cell fusion and microsurgery [4-5], sperm micromanipulation [6], assessment of enzymes [7], and etc. More details can be found in some reviews [8-12].

At present, manipulation in micro/nano meter scale still poses a great challenge to robotics society, which is significantly different from robotics manipulation at macro scale [13-15]. Increasing demands for both accuracy and efficiency in cell manipulation highlight the need for automation process with robotics technology, such as visual servoing [16-17], force feedback [18-19], mechanical modeling of cell in microinjection [20], and motion control [21]. As for optical trapping of micro particles, some works have also been done towards automation to some extent [22-26]. Image processing and path planning in a dynamic environment for cell transportation were reported in our previous work [27]. Generally speaking, however, few works have been done towards manipulation of cells with optical tweezers in dynamic liquid environment together with trapping force analyses during dynamic movement.

Qualitative descriptions of the operation of gradient trap were given in [28-32], which were mainly based on static analysis without considering the cell's motion. The work [25] considered the cell's motion in analyzing the trapping force, but assumed that the cell moved with a constant velocity. In practical application, the cell's velocity in point-to-point movement must be time varying, especially when the moving distance is very small. Accordingly, the assumption of a constant velocity profile does not match the actual situation. Proper design of the velocity profile is important, since it relates to the features of trapping force and laser power closely. Failure to deal with the relationship among the cell moving velocity, trapping force and laser power may cause sequences like cell escaping from the trap, damage of cell, low manipulating efficiency, inaccurate trapping force measurement, and so on.

In this paper, we analyze the dynamic movement of the trapped cell and then obtain proper motion parameters. Based on this analysis, the velocity profile of cell moving can be designed with an optimal moving path computed by a modified A-star algorithm, to ensure safety and efficiency of the cell manipulation progress. Experiments show that the cell can be transported successfully using the proposed motion planning algorithm.

This work was supported by a grant from Research Grants Council of the Hong Kong Special Administrative Region, China [Reference No. CityU 120709], UGC special equipment grant [SEG_CityU01], and a grant from City University of Hong Kong [Reference no. 9360131]

Y. H. Wu and Y. H. Tan are with the Mechanics and Automation Group, Suzhou Research Center of City University of Hong Kong and University of Science and Technology of China, Suzhou, China (e-mail: {wyanhua2, youhuatan2}@student.cityu.edu.hk, Tel: 86-512-87161280).

Dong Sun is with the Department of Manufacturing Engineering and Engineering Management, City University of Hong Kong, Kowloon, Hong Kong (e-mail: medsun@cityu.edu.hk).

W. H. Huang is with the Department of Precision Machinery and Precision Instrumentation, University of Science and Technology of China, Hefei, China (e-mail: whuang@ustc.edu.cn).

## II. Manipulation Platform

Fig. 1 shows our cell manipulation system with optical tweezers, installed on a vibration isolation table. The system includes a diode laser (808 nm, 2 W), a CCD camera, a microscope objective, and a precise moving stage (PI M-111.1DG). The beam produced by the laser passes through a beam expander and is reflected by the dichroic mirror. It passes into the microscope and is focused on the sample which is carried by the stage under automated control. The focus of the laser is fixed on the x-y plane, and the relative movement between the trapped cell and the sample holder can be accomplished by an x-y moving stage. The resolution of the motorized stage is 50 nm. The biological objects can be positioned through image processing, which serves as visual feedback to guide the micromanipulation process.

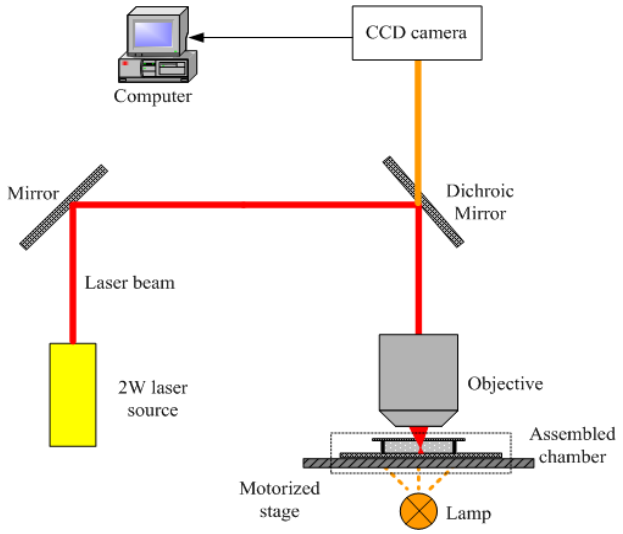


Fig. 1. Cell manipulation system with optical tweezers

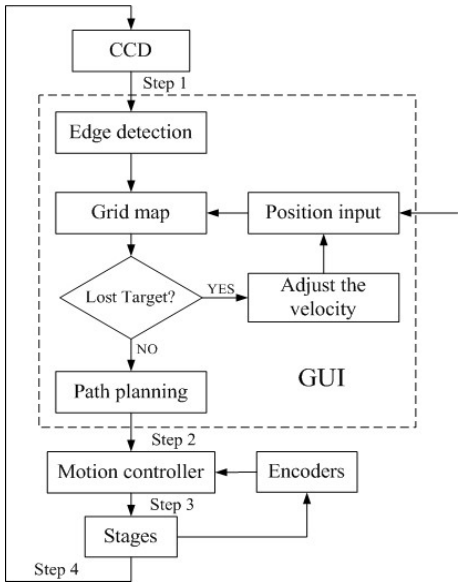


Fig. 2 Hierarchical control of the system.

The motorized stages execute the motion control tasks. Fig. 2 shows the block diagram of the hierarchical control. The control procedures are described as follows:

Step 1: Transmit the original image into a digitalized map in GUI (graphical user interface) with CCD;

Step 2: Compute the path of the cell based on the current and the given terminal states;

Step 3: Send the planned path to motion controller;

Step 4: Acquire new environmental image from CCD.

During this process, the program checks whether the cell is lost in every cycle. If the cell escapes, the trap will go back to the last grid, and the moving velocity will be decreased (usually by 10%).

## III. Trapping Force Analysis in Cell Manipulation

For simplicity, cells with spherical shapes are considered. The theory of ray optics can be used to calculate the trapping force on a dielectric particle with a size that is comparable to the wavelength of the laser. Fig. 3 shows the trapping force produced by a tightly focused laser beam. Stream of photons are presented by a ray of light incident upon the upper side of a cell. The ray is shown refracted and reflected at the upper and the lower surfaces. The effects caused by the stream of photons can be decomposed into axial one (in z-direction) and radical one (in x-directions). The deviation of the cell from the laser focus in z direction can be neglected because of the balance of the gravity and the buoyancy. Therefore, the motion of the trapped cell is mainly considered in x-y plane. With the force analysis in [32], the reflection and refraction of each incident ray contributes to the net radial force on the surface of the cell. The total radial force $F_{trap}$ on the cell is the sum of contributions due to the reflected ray and large number of refracted rays of the incident laser beam.

Fig. 4 illustrates the radial trapping forces with different laser powers imposing on the cell. Denote $x$ as a generalized coordinate representing the deviation of the cell from the center of the trap. The radial trapping force $F_{trap}$ is zero when the cell is perfectly centered in the laser beam. The trapping force pulls the cell back to the center of the beam when $x$ is not zero. The force is also zero when the deviation $x$ is so large that the sphere is completely outside the photo stream. The detailed analysis of the trapping force was given in [28-32]. For simplicity, the relationship between the trapping force $F_{trap}$ and the deviation $x$ is approximated by a linear relation as [8]

$$F_{trap} = kx \qquad |x| < x_0 \tag{1}$$

where $k$ denotes the trapping stiffness, and $x_0$ is the critical deviation when the trapping force begins to decrease.

Fig. 5 illustrates the trapping force versus the deviation $x$ obtained from a simulation on a yeast cell with different radius R. It is demonstrated that the trapping stiffness (slope of the curve) decreases as the radius increases in the range of $|x| < x_0$, which explains why it is more difficult to move large cells than the small cells by optical tweezers in experiments. The parameters of Figs. 4 and 5 are as follows:

$$\rho_s = 1.057 \text{ g/ml},\ \rho_0 = 1.0 \text{ g/ml},\ n_s = 1.54,$$
$$n_0 = 1.33,\ W_0 = 1.5\ \mu m\ ,\ z = 0$$

where $\rho_s$ and $\rho_0$ are the densities of the cell and the ambient material respectively, $n_s$ and $n_0$ are the refractive indexes respectively, $W_0$ is the radius of the beam waist, and z is the distance from the cell to the minimum beam waist [32].

In addition to the trapping force, the flow fluid also exerts a drag force on the trapped cell during cell moving, as shown in Fig. 3. According to Stokes' law [9], the drag force can be expressed by

$$F_{drag} = \frac{6\pi\eta RV}{1-\frac{9}{16}(R/h)+\frac{1}{8}(R/h)^3-\frac{45}{256}(R/h)^4-\frac{1}{16}(R/h)^5} \quad (2)$$

where $R$ is the radius of the cell, $\eta$ is the fluid viscosity ($\eta = 1.01\times10^{-3}\ Pa\cdot s$ at $25^{\circ}C$ for water), $h$ is the separation depth of the cell from the slide, and $V$ is the relative velocity of the trapped cell with respect to the fluid, denoted by

$$V = V_{fluid} - \dot{x}$$

where $V_{fluid}$ is the velocity of the flow. In our study, $V_{fluid}$ is equivalent to the cell moving velocity achieved by the motorized stage. The typical dragging force is less than 10 pN when the velocity is ranged from 10 $\mu m/s$ to 50 $\mu m/s$ .

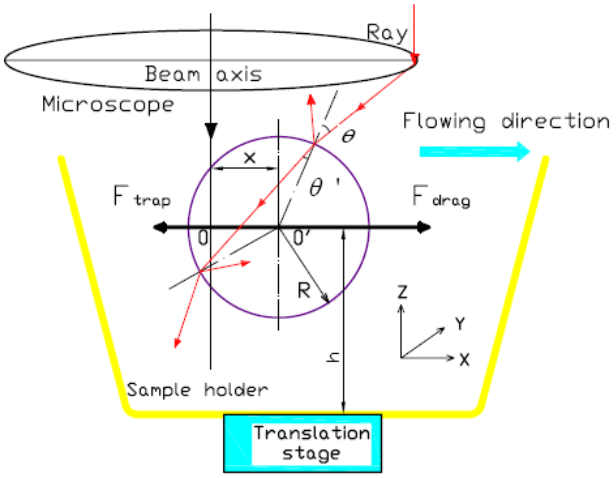


Fig. 3 Force analysis at the cell center with distance $x$ from the beam focus.

Based on typical periodic velocity profiles as shown in Fig. 6, we have the relative velocity as follows

$$V = \begin{cases} a_m t - \dot{x}, & t \le T_0/2 \\ -a_m(t-T_0) - \dot{x}, & T_0/2 < t \le T_0 \end{cases} \quad (3)$$

where $a_m$ is the acceleration of the translation stage which can be designed by the user, and $T_0$ is the time spent to complete a single step motion.

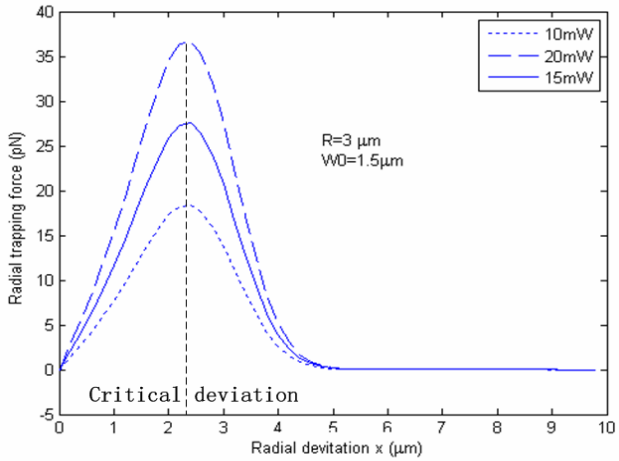


Fig. 4 Radial force versus radial deviation with different laser power. It confirms that the trapping force at the same deviation increases as the laser power increases (ranged from 0 to the critical deviation $x_0$ ).

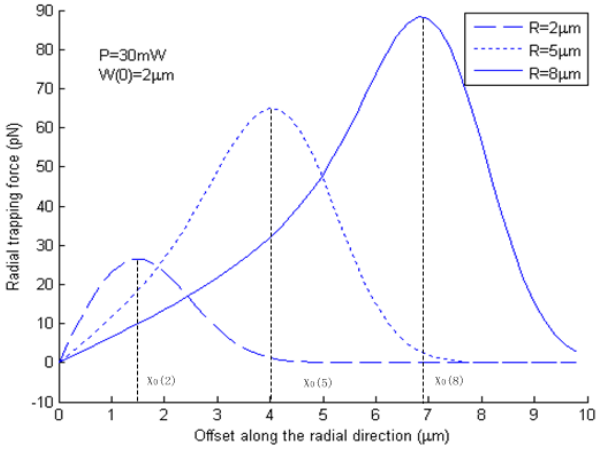


Fig. 5 Radial force versus radial deviation with different size of the cells.

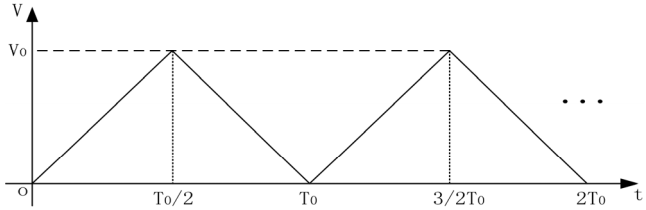


Fig. 6 The periodic velocity profile of the translation stage.

As shown in Fig. 3, the dynamics equation of the motion of the cell is

$$m\ddot{x} = F_{drag} - F_{trap} \quad (4)$$

where $m$ is the mass of the cell. Substituting (1)-(3) into (4), the deviation $x$ can be solved based on the acceleration $a_m$ .

We fit the trapping force to be linear with the stiffness $k = 5\times10^{-6}\ N/m$ (P= 10 mW), which is ranged from -2.3 $\mu m$ to 2.3 $\mu m$ . The deviation $x$ of the cell with different periodic moving distance, denoted by $s_0$ , can be computed based on the acceleration $a_m$ , as shown in Fig. 7.

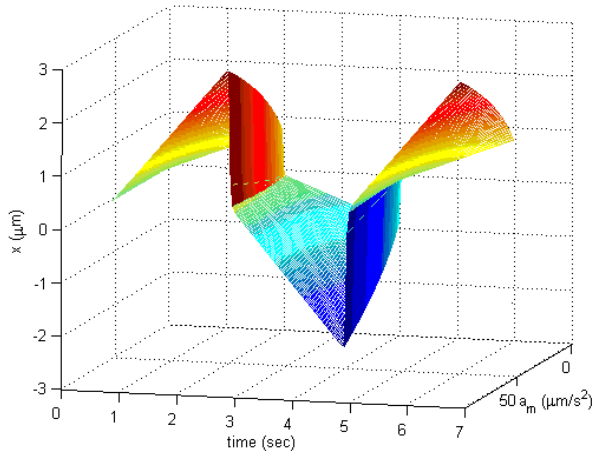


(a) Deviation of the trapped cell with periodic moving distance $s_0$ =30 $\mu m$ .

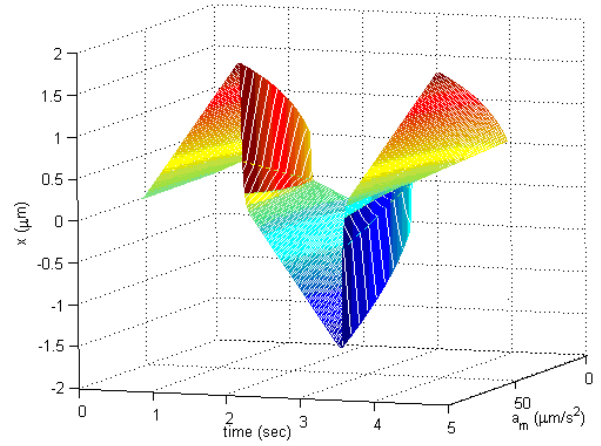


(b) Deviation of the trapped cell with periodic moving distance $s_0$ =15 $\mu m$

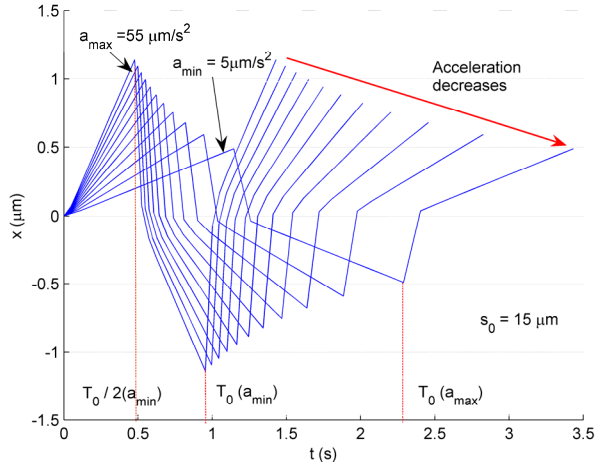


(c) Deviation with periodic moving distance of $s_0$ =15 $\mu m$

Fig. 7 Simulation of the trapped cell versus time (from 0 to 1.5 $T_0$ ), acceleration $a_m$ (from 5 $\mu m/s^2$ to 55 $\mu m/s^2$ ) and moving distance ( $s_0$ ) of the stage.

It is seen from Fig. 7 that the deviation $x$ depends on the acceleration of the translation stage $a_m$ (which is varied from 5 $\mu m/s^2$ to 55 $\mu m/s^2$ ) and the periodic moving distance $s_0$ . The maximum deviation occurs at the time $t = nT_0 / 2$ , where $T_0 = 2\sqrt{s_0 / a_m}$ and n is integer, and the viscous drag force has the maximum value at this time. Then the moving velocity begins to decrease, and the deviation becomes smaller.

As shown in Fig. 4, the trapping force decreases quickly when the deviation $|x| > x_0 = 2.3\ \mu m$ . Therefore, the maximum deviation should ideally be within the range of $x_0$ ; otherwise, the cell may escape due to small trapping force acted on it. Fig. 7 (a) shows that the deviation could exceed 2.3 $\mu m$ if $a_m$ >50 $\mu m/s^2$ in the velocity profile in Fig. 6, when $x_0$ = 30 $\mu m$ . As shown in Fig. 7(b) and (c), the maximum deviation becomes much smaller when the moving distance $s_0$ is 15 $\mu m$ . The moving step $s_0$ is dependent on the environmental factors around the trapped cell, such as obstacle distribution, distance to destination, etc. The motion parameters should be designed by taking balance between practical circumstance and the efficiency.

In the experiments, we successfully transported the yeast cell by selecting $a_m = 20\ \mu m/s^2$ and $s_0 = 30\ \mu m$ . In a few occasions, the cell escaped from the trap after moving a short distance. The success rate of the cell transportation is about 80%. The reasons for failure include collision with fast moving obstacles, improper parameters of the image processing, and that the trapped cell sticks to the slip. In addition, it was found that the cell escaped more easily at the waypoints. Therefore, we should reduce the operation time by selecting a short path, and try to reduce the number of waypoints in the trajectory path.

## IV. Path Planning

When moving the trapped cell, some other cells that locate between the origin and the destination may block the path. Since the laser beam produces the force around its focus, it must keep a distance from the other cells. Therefore, a path-planning algorithm must be designed. Prior to designing the path, the following works must be done.

First, the images from the CCD camera should be changed into binary image, as stated in step 1 of the control procedures in section 2. The ideal effect is attained by adjusting the bars to change the parameters of the canny and dilation algorithms.

Second, the whole moving area is divided into a square grid for simplicity. The grid has two important functions. One is to determine the length of each moving step, and the other is to judge whether the squares can be passed through. The size of the square depends on the safe distance between the trapped cell and others (obstacles), and the safe distance depends on the power of laser and the property of the trapped cell. Since the obstacle particles vibrates all the time, the grid map of the workplace in view must be updated in every step. At the same time, the step length and the moving speed affect the stability of the trapped cell as demonstrated in the last

section.

A modified A-star path planning algorithm is used in this study. A-star algorithm is one of the most classical heuristic path planning algorithms, which searches the path between the starting point and the destination with the lowest cost [33]. In the dynamic environment that contains many cells, the optimal path is determined by computing the path with the lowest cost in every step. Additionally, we smooth (or simplify) the path by decreasing the waypoints. The reason is that at the way point, the cell still moves for a certain distance along previous direction because of its inertia, but the moving direction of the trap changes, which may cause the cell to escape from the trap.

To solve this problem, we modify the A-star algorithm by adding an additional term to the movement cost $F(i,j)$, to penalize the nodes where the moving direction changes. The algorithm for cost estimation can be expressed as:

$$F(i,j) = G(i,j) + H(i,j) + \eta(i,j) \tag{5}$$

where $F(i,j)$ denotes the total moving cost at the given node $(i,j)$, $G(i,j)$ denotes the moving cost from the starting point to the node $(i,j)$, and $H(i,j)$ denotes the estimated moving cost from the given node $(i,j)$ to the final destination. Note that $\eta(i,j)$ is an additionally added moving cost in this study. If there is a waypoint from the note $(i,j)$ to the next position, the value of $\eta(i,j)$ is more than 0; otherwise it is 0. The value of $\eta$ is determined by taking the balance between the smoothness and the moving cost. Increment of $\eta$ reduces the number of the waypoints but may increase the cost. Fig. 8 shows a comparison between the generated paths with different additional value $\eta$, where the cost of moving a single grid in $x$ or $y$ direction was set as 10.

It is seen from Fig. 8(a) that by the standard A-star algorithm there are many waypoints in the path, which is not good to optical trapping. When using the modified A-star algorithm with the additional term $\eta$=10, as is shown in (b), the number of waypoints descreases to two, and the path becomes much smoother than in (a). If $\eta$ increases to 100, as shown in (c), there is only one waypoint, but the movement cost is much greater than in (b). Through a series of tests on the yeast cells, we found that $\eta$ was ideally ranged between 5 and 25 in our experiments.

Fig. 9 illustrates path generation with the modified A-star algorithm ($\eta$=20) in the experiment of moving a yeast cell with optical tweezers. The moving direction was either along x and y axes, or at an angle of $45^o$. To obtain a good image processing effect, we set the moving step as $s_0$=30 $\mu m$ when moving at the angle of $45^o$, as shown in Fig. 9. When moving along $x$ or $y$ direction, the moving step is smaller ($s_0/\sqrt{2}$). According to the computation in section III, the acceleration $a_m$ of the stage should be no more than 50 $\mu m/s^2$. Considering the Brownian motion of the trapped cell and the fluctuation of the envoironment around the cell, the acceleration was set as 15 $\mu m/s^2$ in the experiments. Fig. 10 shows the course of the yeast cell manipulation process in following the generated path. It took about 10 seconds to accomplish the transportation.

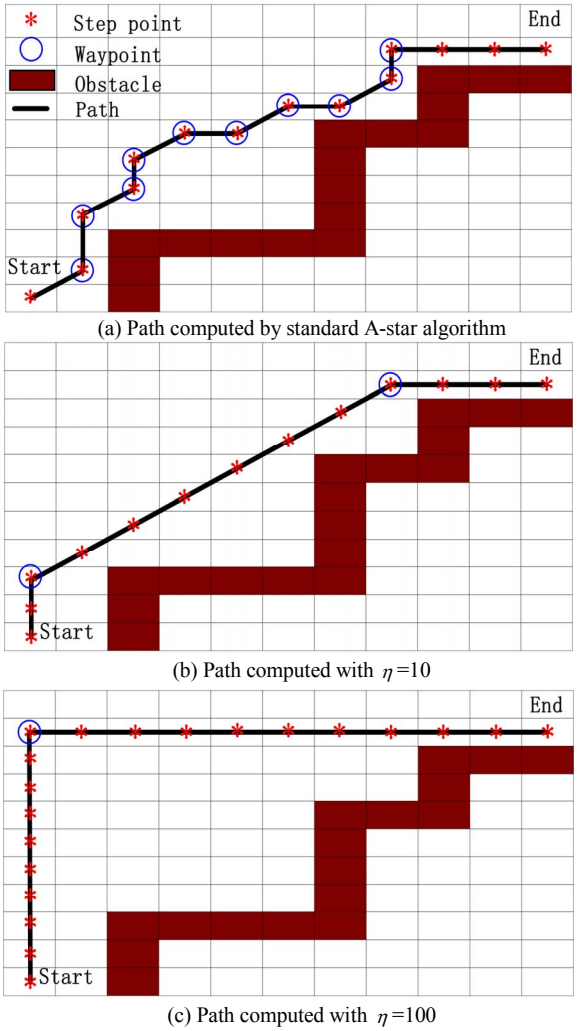

(a) Path computed by standard A-star algorithm

(b) Path computed with $\eta$=10

(c) Path computed with $\eta$=100

Fig. 8 Path generation with standard and modified A-star algorithms.

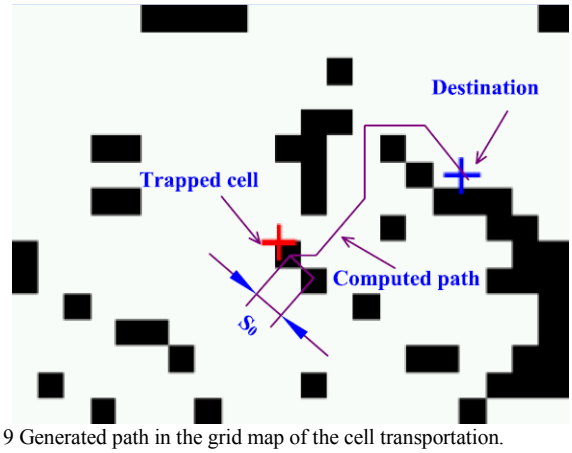

Fig. 9 Generated path in the grid map of the cell transportation.

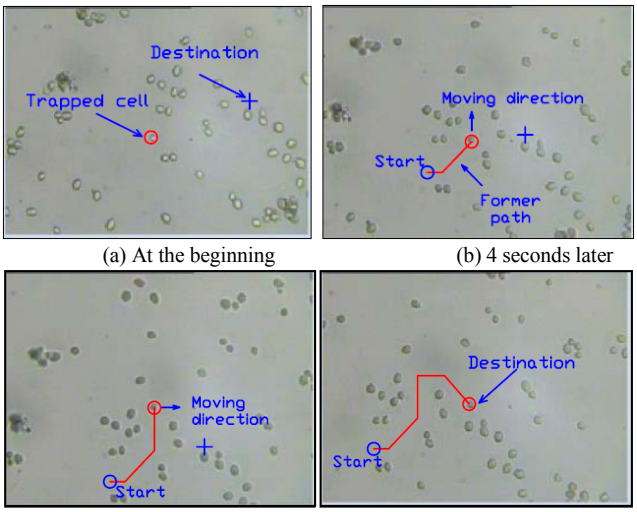


(a) At the beginning (b) 4 seconds later

(c) 6 seconds later (d) 10 seconds later

Fig. 10 Course of transporting the yeast cell to the destination.

## V. CONCLUSION

There is a demand for designing a methodology to manipulate biological cells effectively and safely using a robotic manipulation system with optical tweezers. In this paper, we analyze the dynamics of the trapped cell in movement, and obtain proper motion parameters for motion planning to ensure the safety and efficiency of the cell delivery. A modified A-star path-planning algorithm, which promises low cost and smoothness, is integrated into the manipulation system for automation process. Experiments verify the validity of the proposed manipulation approach.

## REFERENCES


[1] A. Ashkin, "Acceleration and trapping of particles by radiation pressure", *Phys. Rev. Lett*., vol. 24, pp. 156-159, 1970.

[2] A. Ashkin, "History of optical trapping and maniupulation of small-neutral particles, atoms, and molecules", *J. Quantum Elec*., vol. 6, pp. 841-859, 2000.

[3] S. Andreas and W. H. Stefan, "Heating by absorption in the focus of an objective lens", *Opt. Lett*., vol. 23, pp. 325-327, 1998

[4] R. Steubling, S. Cheng, and M. W. Berns, "Laser-induced cell fusion in combination with optical tweezers: The laser-cell fusion trap", *Cytometry,* vol. 12, pp. 505-510, 1991

[5] H. Liang, W. H. Wright, and M. W. Berns, "Micromanipulation of chromosomes in PTK2 cells using laser microsurgery in comination with laser-induced optical forces", *Exp.Cell Res*, vol. 204, pp. 110-120, 1993.

[6] B.Shao, and J. M. Nascimento, "Automated motile cell capture and analysis with optical traps", *Methods in cell biolog*, vol. 82, pp. 602-629, 2007.

[7] K. Svoboda, C. F. Schmidt, and S. M. Block, "Direct observation of kinesin stepping by optical-trapping interferometry", *Nature*, vol. 365, pp. 721-727, 1993.

[8] M. W. Berns, W. Wright, and R. W. Steubing, "Laser microbeam as a tool in cell biology", *Int.Rev.Cytol*, vol. 129, pp. 1-44., 1991.

[9] M. B, S. M. Block, and K. Svoboda, "Biological applications of optical forces", *Annu.Rev.Biophys.Biomol.Struct*, vol. 23, pp. 247-332, 1994.

[10] S. Ermilov, "Dynamic measurement of transverse optical trapping force in biological applications", *Annals of biomedical engineering*, vol. 32, pp. 1016-1026, 2004.

[11] S. C. Kuo, "Using optics to measure biological forces and mechanics", *Traffic*, vol. 2, pp. 757-763, 2001

[12] G. Weber, and K.O. Greulich, "Manipulation of cells, organelles, and genomes by laser microbeam and optical trap", *Int.. Rev. Cytol*, vol. 133, pp. 1-41, 1992.

[13] D. Sun, J. K. Mills and Y. H. Liu, "Position control of robot manipulators manipulating a flexible payload," *Int. J. of Robotics Research*, vol. 18, no. 3, pp. 319-332, Mar. 1999.

[14] Y. H. Liu and D. Sun, "Stabilizing a flexible beam handled by two manipulators via PD feedback," *IEEE Transactions on Automatic Control*, vol. 45, no. 11, pp. 2159-2164, Nov. 2000.

[15] D. Sun and J. K. Mills, "Manipulating rigid payloads with multiple robots using compliant grippers," *IEEE/ASME Trans. on Mechatronics*, vol. 7, no. 1, pp. 23-34, Mar. 2002.

[16] H. Huang, D. Sun, J. K. Mills, W. J. Li, and S. H. Cheng, Visual-based impedance control of out-of-plane cell injection systems, *IEEE Tran. on Automation Science and Engineering*, vol. 6, pp. 565-571, 2009.

[17] H. Huang, D. Sun, J. K. Mills, and S. H. Cheng, 'Robotics cell injection system with vision and force control: Towards automatic batch biomanipulation", *IEEE Trans. on Robotics*, vol. 25, pp. 727-737, 2009.

[18] Y. Xie, D. Sun, C. Liu, S. H. Cheng, and Y. H. Liu, "A flexible force-based cell injection approach in a bio-robotic system", *IEEE Int. Conf. on Robotics and Automation*, Kobe, Japan, pp. 3143-3148, 2009.

[19] B. J. Nelson, J. D. Morrow, and P. K. Khosla, "Robotic manipulation using high bandwidth force and vision feedback", *Mathmatical and computer modeling*, vol. 24, pp. 11-29, 1996.

[20] Y. Tan, D. Sun, W. Huang, and S. H. Cheng, "Mechanical modeling of biological cells in microinjection", *IEEE Trans. on Nanobioscience*, vol. 7, no.4, pp. 257-266, 2008.

[21] S. Huang, and S. Wu, "Vision-based robotics motion control for non-autonomous environment", *J. Intelligent and robotic System*, vol. 54, pp. 733-754, 2008

[22] A. G. Banerjee and S. K. Gupta, "Use of simulation in developing and characterizing motion planning approaches for automated particle transport using optical tweezers", *Virtual Manufacturing Workshop,* Turin, Italy, October, 2008

[23] B. Arvind, and W. L. Thomas, "A flexible system framework for a nanoassembly cell using optical tweezers", *Proceedings of ASME Computers and Information in Engineering Conf.*, pp. 1-10, 2006.

[24] T. N. Buican, .and M. J. Smyth, "Automated single-cell manipulation and sorting by light trapping", *Applied optics*, vol. 26, pp. 5311-5316, 1987.

[25] S. C. Grover, and A. G. Skirtach, "Automated single-cell sorting system based on optical trapping", *J. of Biomedical Optics,* vol. 6, pp. 14-22, 2001.

[26] F. Arai, K. Onda, R. Iitsuka, and H. Maruyama, "Multi-beam laser micromanipulation of microtool by integrated optical tweezers", *IEEE Int. conference on Robotics and Automation*, pp. 1832-1837, 2009.

[27] Y. Wu, D. Sun, W. Huang and Y. Li, "Path planning in automated manipulation of biological cells with optical tweezers", *IEEE Int. Conf. on Control and Automation*, pp. 2021-2026, 2009.

[28] A. Ashkin, J. M. Dziedzic, J. E. Bjorkhom and S. Chu, "Observation of a sngle-beam gradient force optical trap for dielectric particles", *Optics Lett.*, vol. 11, pp. 288-290, 1986.

[29] J. P. Barton, D. R. Alexander, and S. A. Schaub, "Theretical determination of net radiation force and torque for a spherical particle illuminated by a focused laser beam", *J. Appl. Phys.*, vol. 10, pp. 4594-4602, 1989.

[30] R. M. Simmons, J. T. Finer, S. Chu, and J. A. Spudich, "Quantitative measurements of force and using an optical trap", *Biophys. J.,* vol. 70, pp. 1813-1822, 1996.

[31] A. Ashkin, "Forces of a single-beam gradient laser trap on a dielectric sphere in the ray optics regime," *Biophys. J.*, vol. 61, pp. 569-82, 1992

[32] R. C. Gauthier and S. Wallace, "Optical levitation of spheres: analytical development and numerical computations of the force equations", *J. Opt. Soc. Am. B*, vol. 12, pp. 1680-1685, 1995.

[33] B. ChongSeet, and G. Lin, "A-STAR: a mobile ad hoc routing strategy for metropolis vehicular communications", *Networking LNCS*, pp. 989-999, 2004.